


**Excitonic effects on electron spin orientation and relaxation in wurtzite GaN**Shixiong Zhang,<sup>1</sup> Ning Tang<sup>ⓧ,1,3,\*</sup>, Xiaoyue Zhang,<sup>1</sup> Xingchen Liu<sup>ⓧ,1</sup>, Hongming Guan,<sup>1</sup> Yunfan Zhang,<sup>1</sup> Xuan Qian,<sup>2,4</sup> Yang Ji,<sup>2,4</sup> Weikun Ge<sup>ⓧ,1</sup> and Bo Shen<sup>1,3,†</sup><sup>1</sup>State Key Laboratory of Artificial Microstructure and Mesoscopic Physics, School of Physics, Peking University, Beijing 100871, China<sup>2</sup>State Key Laboratory for Superlattices and Microstructures, Institute of Semiconductors, Chinese Academy of Sciences, Beijing 100083, China<sup>3</sup>Frontiers Science Center for Nano-optoelectronics & Collaboration Innovation Center of Quantum Matter, Peking University, Beijing 100871, China<sup>4</sup>College of Materials Science and Opto-Electronic Technology, College of Physical Sciences, University of Chinese Academy of Sciences, Beijing 100049, China (Received 6 July 2020; revised 15 August 2021; accepted 10 September 2021; published 21 September 2021)

Excitonic effects on electron spin orientation and relaxation in wurtzite GaN are investigated with photon-energy-dependent time-resolved Kerr rotation spectroscopy at low temperatures. It is observed that the spin orientation generated with circularly polarized light can be manipulated with photon energy upon the excitation energy being resonated with various fine energy levels in the band structure. Three reversals of the spin orientation and a remarkable reduce of spin relaxation time are obtained, which is caused by the photon-energy dependent transitions from the heavy and light hole bands to the exciton levels and the conduction band edge. A long spin relaxation time of 1.7 ns is attributed to the spin polarization of donor-bound electrons as the formation of donor-bound excitons, while the spin relaxation time of the conduction band electrons is shorter and shows a nonmonotonic dependence on the optical excitation power, revealing the dominant role of the D'yakonov-Perel' spin relaxation mechanism in wurtzite GaN.

DOI: [10.1103/PhysRevB.104.125202](https://doi.org/10.1103/PhysRevB.104.125202)

Due to electric-field controllable spin-orbit coupling (SOC) and potential device applications at room temperature, III-nitride wide bandgap semiconductors have attracted significant interest in the community of semiconductor spintronics [1–4]. Spin injection is one of the key points for semiconductor spintronics. Electrical injection [5–7] and optical injection [8–10] are the two common approaches. Optical spin injection is a simple and powerful way to study fundamental spin properties and achieve novel spintronic device functions.

In order to implementing effective optical spin manipulation and accurate measurements of electron spin relaxation time, a thorough understanding of optical selection rules is imperative, which relates the electron spin orientation with the photon energy and helicity. Circularly polarized light with  $\sigma_-$  or  $\sigma_+$  helicity could be utilized to selectively generate electrons with up or down spin orientation, exactly as that in the case of optical information storage [11]. The photon energy being resonated with various fine energy levels could affect the spin polarization [12,13]. It is worth noting that the intrinsic splitting of the valence subbands in wurtzite GaN [14] may offer a new option for preferentially exciting electrons with single spin orientation and reveal the conditions for efficient optical spin injection. Nevertheless, the electron spin orientation in wurtzite GaN, which may be manipulated with photon energy corresponding to fine band structures,

has rarely been investigated experimentally. On the other hand, the spin dynamics of semiconductors close to the band gap are strongly determined by the fine band structures. In wurtzite GaN, the spin splitting of the conduction band (CB), which is the main source causing the electron spin relaxation, provides a feasible way to modulate the spin relaxation time [8–10]. The shallow bound states introduced by doping donor impurities such as Si in GaN can yield a longer spin relaxation time [9] and improve the electron transport [15], and hence be beneficial for spintronic devices. Besides, the exciton levels near the band edge have a considerable difference in the spin relaxation from the CB due to the large excitonic exchange interaction [16]. Therefore, the shallow bound states and exciton levels close to the CB would create an inherent obstacle for accurate measurements of the CB electrons' spin relaxation time. However, the individual spin dynamics in these fine energy levels has scarcely been distinguished, and it is also interesting to explore the excitonic effects on electron spin relaxation as a fundamental physical question.

Here we use time-resolved Kerr rotation (TRKR) measurements to study the optical selection rules and spin dynamics in a moderately Si-doped GaN. The spectrally resolved spin orientation neatly reveals the individual band structures associated with the exciton levels and shallow states. Due to the large exciton binding energy in wurtzite GaN, the electron spin relaxation at various fine energy levels is well distinguished, comprehensively illustrating excitonic effects on electron spin dynamics.

\*ntang@pku.edu.cn

†bshen@pku.edu.cn

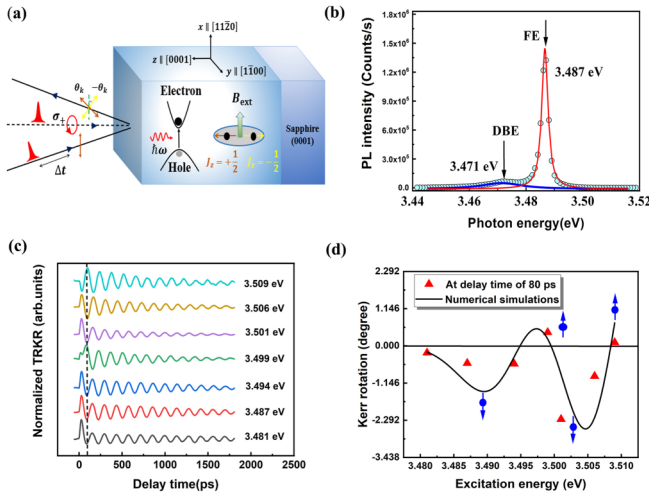


FIG. 1. (a) Schematic diagram of the experimental principle. The sign of Kerr rotation  $\pm\theta_K$  follows from spin orientation  $J_z = \pm 1/2$ . (b) Photoluminescence spectrum of the sample at 8 K and the excitation power larger than 20 mW. (c) TRKR signals of different excitation energy at 10 K and  $B = 0.26$  T. (d) Kerr rotation angles at a delay time of 80 ps extracted from the raw data in Fig. 1(c) and numerical simulations based on the fundamental optical transition.

The wurtzite GaN were grown with metal organic chemical vapor deposition on a *c*-plane sapphire substrate. The epilayer is 2  $\mu\text{m}$  with Si-doping density of  $6 \times 10^{17} \text{cm}^{-3}$ . The TRKR measurements, as shown in Fig. 1(a), were carried out in a temperature range varied from 8 K to 300 K. An external magnetic field was applied in Voigt geometry. The femtosecond pump and probe pulses were supplied with a mode-locked Ti: sapphire laser with a repetition rate of 76 MHz. The probe beam was linearly polarized and delayed by a mechanical time delay line. Meanwhile, the pump beam was modulated periodically to left circularly polarized light  $\sigma_+$  (or right circularly polarized light  $\sigma_-$ ) with a photoelastic modulator. In order to extract the weak spin signals from the background noise, a modulation frequency 50 KHz was set as the reference frequency of a lock-in amplifier. The pumping light spot has a diameter of about 50  $\mu\text{m}$ . On the surface of a spin polarized sample, different reflectivity for different circularly polarized light would induce Kerr rotation  $\theta_K$  of a linearly polarized (probe) beam. The spin relaxation process could then be exhibited by the time-dependent  $\theta_K$ , and the electron spin orientation can be revealed from the sign of  $\theta_K$ .

For the sake of identifying various fine energy levels in the band structure, photoluminescence (PL) spectroscopy measurements were conducted. Two luminescence peaks emerge, as shown in Fig. 1(b). The double-peak Lorentzian fitting for the PL spectrum demonstrates that the photon energies of the peaks' center are 3.471 eV and 3.487 eV, with a full width at half maxima (FWHM) of 17 meV and 3 meV, respectively. Compared with the typical results in Ref. [17], the two peaks at 3.471 eV and 3.487 eV are attributed to the recombination of the donor-bound exciton (DBE) and free exciton (FE), respectively. Additionally, owing to a wider spreading of the donor-bound states in the momentum space [17], the luminescence spectrum of the DBE characterizes with a larger FWHM.

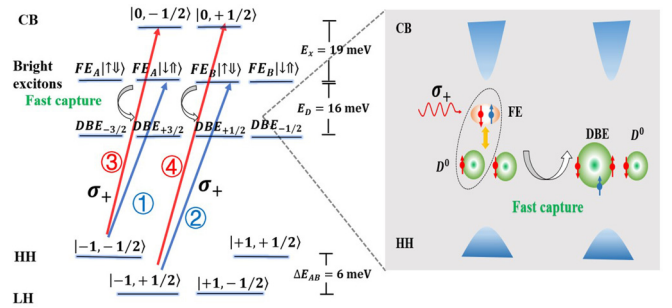


FIG. 2. Schematic diagram of optical transitions under a left circularly polarized light  $\sigma_+$ . The inset describes the fast capture of FE.

In contrast, the momentum of FE concentrates at  $\Gamma$  point, resulting in a smaller FWHM [18]. The energy difference between DBE and FE implies that the donor binding energy  $E_D$  is 16 meV. Given the exciton binding energy  $E_x = 19$  meV [19], the band gap at 8 K is evaluated to be 3.487 eV + 0.019 eV = 3.506 eV. These values are consistent with the experimental and theoretical results in Refs. [17,19,20].

The valence band of wurtzite GaN consists of three doubly degenerate bands: heavy hole band (HH), light hole band (LH), and crystal-field split-off band (CH) [21], while the CB is also a doubly degenerate band. In a surface-incidence geometry on a *c*-plane GaN, as depicted in Fig. 1(a), the optical transition from CH to CB is forbidden [19]. Only the transitions, related to HH and LH, contribute to the spin polarization of photoexcited electrons. To distinguish the fine energy levels, the TRKR measurements were conducted at low temperatures, where the thermal broadening is smaller than the splitting energy between HH and LH ( $\Delta E_{AB} = 6$  meV [19]). Within the accuracy of the experiment, the electron spin precession could merely be detected when the excitation energy is in the range of 3.481 eV to 3.509 eV, as shown in Fig. 1(c). Considering the laser energy broadening of 10 meV, the discrete excitation spectrum in TRKR measurements is consistent with the results from the PL spectrum. Figure 1(d) illustrates the  $\theta_K$  at a delay time of 80 ps as a function of the excitation energy. The spectrally resolved spin optical orientation manifests the fine energy levels in the band structure [12,13].

As depicted in Fig. 2, a left circularly polarized light  $\sigma_+$  with various excitation energies is chosen to excite spin polarization, and four kinds of optical transition are involved. We have omitted the angular momentum units  $\hbar$  in this paper and  $|L_z, m_s\rangle = |+1, +1/2\rangle, |-1, -1/2\rangle, |+1, -1/2\rangle, |-1, +1/2\rangle$  denotes electronic states in the HH (LH) bands, where  $L_z$  and  $m_s$  are the orbital and spin angular momentum, respectively. These optical transitions, obeying energy and angular momentum conserved, lead to the spin polarization of photoexcited electrons. In the process of optical transitions, the photons transfer their angular momentum +1 to the electronic orbital angular momentum. Therefore, the optical transitions “ $|-1, -1/2\rangle \rightarrow |0, -1/2\rangle$ ” and “ $|-1, +1/2\rangle \rightarrow |0, +1/2\rangle$ ” would take place in sequence as the excitation energy increases, leading to the reversal of the sign of  $\theta_K$ . Accounting for the optical

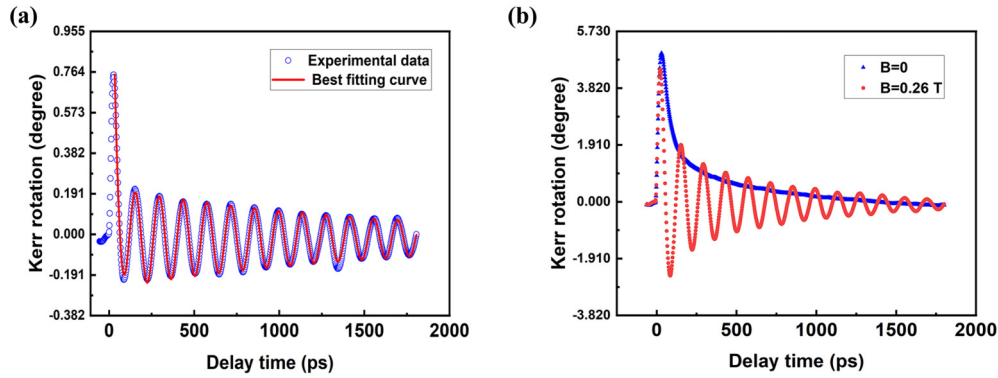
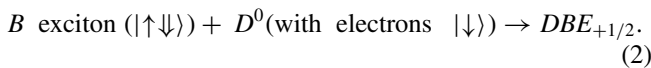
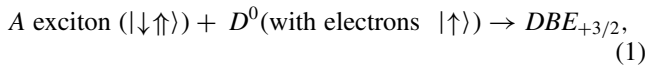


FIG. 3. TRKR signals (in the unit of degree) at the excitation energy of (a) 3.481 eV and (b) 3.501 eV, corresponding to the spin relaxation of donor-bound electrons and CB electrons, respectively.

transitions related to the exciton levels and/or the CB, there are three reversals of the sign of  $\theta_K$ , as illustrated in Fig. 1(d). Numerical simulations accounting for the four kinds of optical transition are in line with the experimental results in Fig. 1(d), which validates that the reversal of the sign of  $\theta_K$  should be attributed to the fine levels in the band structure instead of other optical index effects. It confirms that the spin orientation can indeed be manipulated with the excitation energy. Further, a high spin polarizability may be obtained upon the photon energy selectively exciting electrons from the HH or LH due to the considerable intrinsic splitting of the HH and LH in wurtzite GaN.

In detail, it is derived from Fig. 1(b) that if the excitation energy  $E_{\text{exc}}$  of  $\sigma_+$  satisfies  $3.487 \text{ eV} < E_{\text{exc}} < 3.506 \text{ eV}$ , the photoexcited electron-hole pairs would form either A ( $|\downarrow\uparrow\rangle$ ) or B excitons ( $|\uparrow\downarrow\rangle$ ) due to Coulomb interactions. However, as shown in Fig. 1(c), the signature of excitonic spin relaxation, featured with a spin relaxation time of subpicosecond [22,23], was not obvious. Alternatively, a spin relaxation time of longer than 1 ns was observed, which might stem from donor-bound electrons. That is to say, the excitons are captured immediately by some neutral donors  $D^0$ , such as silicon and oxygen [17]:



For instance, as shown in the inset of Fig. 2, while the photon energy of  $\sigma_+$  coincides with the A exciton transition (the process “①”), the  $D^0$  with electrons  $|\uparrow\rangle$  are combined with the A exciton ( $|\downarrow\uparrow\rangle$ ), leaving more  $D^0$  with electrons  $|\downarrow\rangle$  in the remaining  $D^0$ . It is noted that two electrons of  $DBE_{+3/2}$  have opposite spin in a singlet state [24], and hence make no contribution to spin polarization. Therefore, the carrier spin polarization could come from only two candidates: the holes  $|\uparrow\rangle$  in  $DBE_{+3/2}$  and the donor-bound electrons  $|\downarrow\rangle$  in  $D^0$ . Similarly, for the B exciton transition (the process “②”), the hole  $|\downarrow\rangle$  in  $DBE_{+1/2}$  and  $D^0$  with electrons  $|\uparrow\rangle$  contribute to the carrier spin polarization [24]. Furthermore, once the excitation energy exceeds the band gap, i.e.,  $E_{\text{exc}} > 3.506 \text{ eV}$ , the

electrons are excited to the CB (processes “③”, “④”) because the hot electrons have sufficient energy to escape from the exciton binding state. On the basis of the above analysis, the optical transition processes numbered with “①”, “②”, “③”, and “④” would take place orderly as the excitation energy increases, which coincides with three reversals of the sign of  $\theta_K$  in Fig. 1(d). Besides, when the photon energy is resonating with the exciton levels, the spin relaxation time of the donor-bound electrons is longer than that of the CB electrons, which is also in accord with the photon energy dependence of the spin relaxation time described in the following.

The band structures within various fine energy levels bring about individual spin relaxation behaviors. First, when the pump and probe energies are tuned to make the  $DBE_{+3/2}$  transition labeled with “①”, the holes  $|\uparrow\rangle$  in  $DBE_{+3/2}$  and the donor-bound electrons  $|\downarrow\rangle$  in  $D^0$  would contribute to the total spin polarization. While a transverse magnetic field  $B$  is applied in Vigot geometry, the Larmor precession frequency associated to the carriers is

$$\omega_{e,h} = \frac{g_{e,h}^{\perp} \mu_B}{\hbar} B, \quad (3)$$

where  $g_{e,h}^{\perp}$  is the transverse electron (hole) Landé factor,  $\mu_B$  is the Bohr magneton, and  $\hbar$  is the reduced Planck constant. Whereas the transverse heavy hole Landé factor  $g_h^{\perp}$  is almost zero [25], the magnetic field only induces an electron spin precession. The temporal evolution of total spin polarization can then be described as [26]

$$S_z(t) = A^{DBE} e^{-t/\tau^{DBE}} + A^D e^{-t/\tau^D} \cos(\omega_e t), \quad (4)$$

where the nonoscillatory component represents the spin relaxation of DBE while the oscillatory term signifies the spin relaxation of donor-bound electrons in  $D^0$ ;  $A^{DBE}$ ,  $\tau^{DBE}$  and  $A^D$ ,  $\tau^D$  denote their amplitudes and spin relaxation times, respectively. Here  $\tau^{DBE}$  is the effective spin relaxation time accounting for the recombination and spin relaxation of DBE. As shown in Fig. 3(a), the nonoscillatory component is clearly seen in the TRKR signals at excitation energy of 3.481 eV, at which the excitons are guaranteed to be excited alone. A best fitting with Eq. (4) gives  $\tau^{DBE} = 21 \text{ ps}$  and  $\tau^D = 1715 \text{ ps}$ , respectively.

Second, the CB electrons have a completely different spin relaxation behavior. The spin relaxation dynamics can be

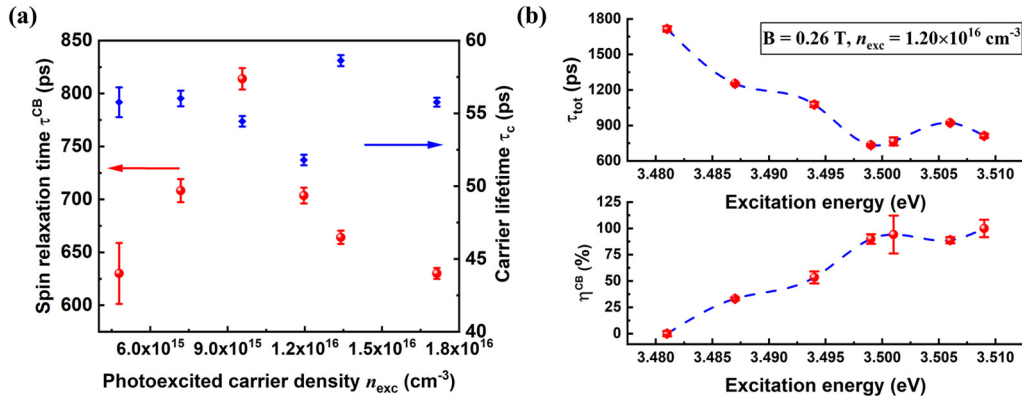


FIG. 4. (a) Carrier density dependence of spin relaxation time and carrier lifetime for CB electrons. (b) Excitation energy dependence of  $\tau^{tot}$  and  $\eta^{CB}$  at  $B = 0.26$  T and  $n_{exc} = 1.20 \times 10^{16} cm^{-3}$ . Dot splines are guides to the eye.

described as [8]

$$S_z(t) = (A_1 e^{-t/\tau_c} + A_2) e^{-t/\tau^{CB}} \cos(\omega_e t), \quad (5)$$

where  $\tau_c$  is the carrier lifetime, and  $\tau^{CB}$  denotes the spin relaxation time of CB electrons. The total amplitude is divided into two parts:  $A_1$  is the amplitude of the spin polarized electrons which undergo both a process of recombination with holes and the intrinsic spin relaxation;  $A_2$  is the amplitude of the spin polarized electrons undergoing the intrinsic spin relaxation alone. Figure 3(b) shows the TRKR signals at the excitation process labeled with “③.” Obviously, the nonoscillatory component associated with DBE spin relaxation disappears. From the fitting with Eq. (5),  $\tau^{CB} = 630$  ps and  $\tau^{CB} = 674$  ps are derived in the case of  $B = 0$  and  $B = 0.26$  T, respectively. The increase of the spin relaxation time under external magnetic field results from the anisotropy of SOC in wurtzite GaN under the framework of D’yakonov-Perel’ mechanism [10]. It is found that the carrier lifetime of 55 ps is nearly independent of the external magnetic field and excitation power.

Moreover, it is observed that the spin relaxation time of the CB electrons shows a nonmonotonic dependence on the photoexcited carrier density  $n_{exc}$ , as depicted in Fig. 4(a). The spin relaxation time reaches maximum around  $n_{exc} = 9.57 \times 10^{15} cm^{-3}$ . It has been confirmed that the electron-electron and electron-impurity scatterings could contribute to the nonmonotonic density dependence of the spin relaxation time, while electron-electron scattering could be significant in a high mobility sample [27]. However, the mobility of our sample is about  $9.17 cm^2/V s$ , according to the Van der Pauw measurements, indicating that electron-electron scattering could be insignificant in our sample. The nonmonotonic dependence could be explained well by the D’yakonov-Perel’ mechanism, similar to the theoretical description about doping density effect on spin relaxation by Buß *et al.* [9]. The tensor of the DP spin relaxation rate is described as

$$\gamma_{ij} = \langle \Omega_{eff}^2 \rangle \tau_p, \quad (6)$$

where  $i, j = x, y, z$ ;  $\langle \Omega_{eff}^2 \rangle$  is the average effective magnetic field induced by the SOC;  $\tau_p$  is the momentum scattering time affected by electron-impurity scattering.  $\langle \Omega_{eff}^2 \rangle$  and  $\tau_p$  have a various dependence of the carrier density in the nondegenerate and degenerate regime, resulting in a longest spin relaxation

time at a critical carrier density  $n_c$ . In the nondegenerate regime,  $\langle \Omega_{eff}^2 \rangle$  varies weakly with the carrier density. With increasing carrier density, the momentum scattering time  $\tau_p$  reduces since the Coulomb screen effect becomes more pronounced in electron-impurity scattering [27,28], then the spin relaxation becomes slower. Instead, in the degenerate regime,  $\langle \Omega_{eff}^2 \rangle$  increases with density due to the occupation of higher  $k$  states, while the momentum scattering time  $\tau_p$  is approximately independent of the carrier density due to the saturation of the Coulomb screen effect, then the spin relaxation gets faster. Theoretically, a peak of the spin relaxation time occurs at the critical carrier density  $n_c = 1.03 \times 10^{16} cm^{-3}$ , determined via

$$k_B T = (3\pi^2 n_c)^{2/3} \hbar^2 / 2m^*, \quad (7)$$

where  $k_B$  is the Boltzmann constant,  $m^* = 0.2 m_e$  is the effective mass in wurtzite GaN [29], and  $m_e$  is the free electron mass. In our sample, the carrier density is the sum of the donor-ionized and photoexcited electron density. It must be noted that the donors are hardly ionized at 10 K, and the ionized carrier density can be estimated via  $n_{ion} \approx N_D \exp(-E_D/k_B T) = 5.27 \times 10^9 cm^{-3}$  and thus be ignored. The density of photoexcited carriers is estimated via [30]

$$n_{exc} = (1 - R)[1 - \exp(-\alpha d_s)] P_{exc} / (A f_{rep} \hbar \omega_{exc} d_s), \quad (8)$$

where  $R$  is the combined reflectivity of the cryostat window and sample,  $\alpha = 8 \times 10^4 cm^{-1}$  is the absorption coefficient [31],  $d_s$  is the epilayer thickness,  $A$  is the area of the pump spot, and  $f_{rep}$  and  $\hbar \omega_{exc}$  are the repetition frequency and photon energy of the pump beam, respectively. Therefore, the critical density  $n_{exc} = 9.57 \times 10^{15} cm^{-3}$  in our experiment conforms well with the theoretical result above. It is concluded then that the spin relaxation of CB electrons is dominated by the D’yakonov-Perel’ mechanism, where the electron-impurity scattering plays the key role.

Finally, the extracted spin relaxation time from spectrally resolved TRKR signals reduces remarkably with increasing excitation energy, as illustrated in Fig. 4(b). It may result from the fact that the spin-polarized CB electrons and donor-bound electrons are excited simultaneously due to the inevitable laser broadening. Then the spin relaxation rate can be estimated

via [32]

$$\frac{1}{\tau_{\text{tot}}} = \eta^D \frac{1}{\tau^D} + \eta^{CB} \frac{1}{\tau^{CB}}, \quad (9)$$

where  $\eta^D$  and  $\eta^{CB}$  are the percentages of donor-bound electrons and CB electrons, respectively. Figure 4(b) also shows  $\eta^{CB}$  as a function of the excitation energy. The spin relaxation of the CB electrons becomes dominant as the excitation energy reaching the band gap. Therefore, we believe that the remarkable decrease of the spin relaxation time is induced by the transition from the spin relaxation of donor-bound electrons to that of CB electrons.

In conclusion, the impact of the band structures covering various fine energy levels on spin optical orientation and relaxation has been carefully investigated with photon-energy dependent TRKR. It is observed that the spin orientation generated with circularly polarized light could be manipulated with photon energy upon the excitation energy being resonated with various fine energy levels. Due to the individual band structure associated with the large exciton binding

energy and shallow impurity states in wurtzite GaN, three reversals of the spin orientation and a remarkable reduction of the spin relaxation time were obtained. A long spin relaxation time of 1.7 ns is attributed to the spin polarization of donor-bound electrons indicating that the photoexcited FE would be captured to form DBE, while the spin relaxation time of the conduction band electrons is shorter and shows a nonmonotonic dependence on the optical excitation power, exhibiting the dominant role of D'yakonov-Perel' spin relaxation mechanism in wurtzite GaN. These experimental finds are conducive to implement spin manipulation with optical means, in favor of possible applications for GaN-based spintronic devices and quantum information processes.

This work was supported by the National Key Research and Development Program of China (Grants No. 2018YFB0406603, No. 2018YFE0125700, and No. 2016YFA0301202), the National Natural Science Foundation of China (Grants No. 61574006, No. 61522401, No. 61927806, No. 61521004, No. 11634002, and No. 11674311), and the K. C. Wong Education Foundation, China.

- 
- [1] H. J. Chang, T. W. Chen, J. W. Chen, W. C. Hong, W. C. Tsai, Y. F. Chen, and G. Y. Guo, *Phys. Rev. Lett.* **98**, 136403 (2007).
- [2] X. W. He, B. Shen, Y. Q. Tang, N. Tang, C. M. Yin, F. J. Xu, Z. J. Yang, G. Y. Zhang, Y. H. Chen, C. G. Tang, and Z. G. Wang, *Appl. Phys. Lett.* **91**, 071912 (2007).
- [3] N. Tang, B. Shen, K. Han, F.-C. Lu, F.-J. Xu, Z.-X. Qin, and G.-Y. Zhang, *Appl. Phys. Lett.* **93**, 172113 (2008).
- [4] C. Yin, B. Shen, Q. Zhang, F. Xu, N. Tang, L. Cen, X. Wang, Y. Chen, and J. Yu, *Appl. Phys. Lett.* **97**, 181904 (2010).
- [5] T.-E. Park, Y. H. Park, J.-M. Lee, S. W. Kim, H. G. Park, B.-C. Min, H.-J. Kim, H. C. Koo, H.-J. Choi, S. H. Han, M. Johnson, and J. Chang, *Nat. Commun.* **8**, 15722 (2017).
- [6] A. Bhattacharya, M. Z. Baten, and P. Bhattacharya, *Appl. Phys. Lett.* **108**, 042406 (2016).
- [7] S. Jahangir, F. Dogan, H. Kum, A. Manchon, and P. Bhattacharya, *Phys. Rev. B* **86**, 035315 (2012).
- [8] J. H. Buß, J. Rudolph, F. Natali, F. Semond, and D. Hägele, *Phys. Rev. B* **81**, 155216 (2010).
- [9] J. H. Buß, J. Rudolph, S. Starosielec, A. Schaefer, F. Semond, Y. Cordier, A. D. Wieck, and D. Hägele, *Phys. Rev. B* **84**, 153202 (2011).
- [10] J. H. Buß, J. Rudolph, F. Natali, F. Semond, and D. Hägele, *Appl. Phys. Lett.* **95**, 192107 (2009).
- [11] M. Kroutvar, Y. Ducommun, D. Heiss, M. Bichler, D. Schuh, G. Abstreiter, and J. J. Finley, *Nature (London)* **432**, 81 (2004).
- [12] S. Pfalz, R. Winkler, T. Nowitzki, D. Reuter, A. D. Wieck, D. Hägele, and M. Oestreich, *Phys. Rev. B* **71**, 165305 (2005).
- [13] S. Pfalz, R. Winkler, N. Ubbelohde, D. Hägele, and M. Oestreich, *Phys. Rev. B* **86**, 165301 (2012).
- [14] C. Brimont, M. Gallart, A. Gadalla, O. Cregut, B. Hoenerlage, and P. Gilliot, *J. Appl. Phys.* **105**, 023502 (2009).
- [15] D. G. Zhao, H. Yang, J. J. Zhu, D. S. Jiang, Z. S. Liu, S. M. Zhang, Y. T. Wang, and J. W. Liang, *Appl. Phys. Lett.* **89**, 112106 (2006).
- [16] T. Ishiguro, Y. Toda, and S. Adachi, *Appl. Phys. Lett.* **90**, 011904 (2007).
- [17] G. Pozina, S. Khromov, C. Hemmingsson, L. Hultman, and B. Monemar, *Phys. Rev. B* **84**, 165213 (2011).
- [18] D. Kovalev, B. Averboukh, D. Volm, B. K. Meyer, H. Amano, and I. Akasaki, *Phys. Rev. B* **54**, 2518 (1996).
- [19] G. D. Chen, M. Smith, J. Y. Lin, H. X. Jiang, S. H. Wei, M. A. Khan, and C. J. Sun, *Appl. Phys. Lett.* **68**, 2784 (1996).
- [20] W. Gotz, N. M. Johnson, C. Chen, H. Liu, C. Kuo, and W. Imler, *Appl. Phys. Lett.* **68**, 3144 (1996).
- [21] S. H. Wei and A. Zunger, *Appl. Phys. Lett.* **69**, 2719 (1996).
- [22] T. Kuroda, T. Yabushita, T. Kosuge, A. Tackeuchi, K. Taniguchi, T. Chinone, and N. Horio, *Appl. Phys. Lett.* **85**, 3116 (2004).
- [23] C. Brimont, M. Gallart, O. Cregut, B. Honerlage, and P. Gilliot, *Phys. Rev. B* **77**, 125201 (2008).
- [24] J. Tribollet, E. Aubry, G. Karczewski, B. Sermage, F. Bernardot, C. Testelin, and M. Chamarro, *Phys. Rev. B* **75**, 205304 (2007).
- [25] C. Y. Hu, K. Morita, H. Sanada, S. Matsuzaka, Y. Ohno, and H. Ohno, *Phys. Rev. B* **72**, 121203(R) (2005).
- [26] G. Garcia-Arellano, F. Bernardot, G. Karczewski, C. Testelin, and M. Chamarro, *Phys. Rev. B* **99**, 235301 (2019).
- [27] J. H. Jiang and M. W. Wu, *Phys. Rev. B* **79**, 125206 (2009).
- [28] M. W. Wu, J. H. Jiang, and M. Q. Weng, *Phys. Rep.* **493**, 61 (2010).
- [29] S. Shokhovets, G. Gobsch, and O. Ambacher, *Appl. Phys. Lett.* **86**, 161908 (2005).
- [30] J. H. Buß, T. Schupp, D. J. As, D. Hägele, and J. Rudolph, *J. Appl. Phys.* **126**, 153901 (2019).
- [31] G. Y. Zhao, H. Ishikawa, H. Jiang, T. Egawa, T. Jimbo, and M. Umeno, *Jpn. J. Appl. Phys.* **38**, L993 (1999).
- [32] N. J. Harmon, W. O. Putikka, and R. Joynt, *Phys. Rev. B* **81**, 085320 (2010).